USE OF VIBRATION DATA FOR RAILWAY TRACK CONDITION ASSESSMENT VIA MOBILE PLATFORMS

Ergashev Qahramon Xushvaktovich

Tashkent state Transport university, Tashkent, Uzbekistan.

sharingam@mail.ru

Abstract. The article presents a comprehensive framework for railway track diagnostics based on the analysis of vibration signals. The principal objective of the study is to acquire detailed, data-driven insights into the actual technical condition of railway infrastructure through a passive experimental approach. This is achieved by utilizing mobile diagnostic platforms and advanced measurement techniques designed to assess the structural state of the track without interrupting regular rail operations. The research outlines the full spectrum of diagnostic procedures carried out in accordance with established railway regulations and emphasizes the advantages and operational capabilities of mobile diagnostics within railway transport systems.

Keywords: Railway transport, On-board monitoring (OBM), Rail defects, Vibration diagnostics, Mobile measurement platform, Structural health monitoring, Track condition assessment.

1. Introduction

Ensuring that railway lines meet appropriate quality standards, particularly in terms of track geometry and surface element diagnostics, is a key responsibility for infrastructure managers. Adherence to these standards is essential not only to guarantee safe operations but also to maintain passenger comfort. In Uzbekistan, statistics from the Office of Rail Transport indicate a steady increase in rail traffic, which accelerates the degradation of infrastructure components. This results in intensified fatigue processes, faster wear, and an increased risk of safety-critical failures.

2. Research methodology

2.1. Mobile measurement platform

For the purposes of this study, two mobile diagnostic configurations were employed on selected railway routes (see Section 3.2). The first configuration (Set A) consisted of a measurement platform of type Xk 03–0517 coupled with a rail vehicle DH–350.11 (Fig. 1). The second configuration (Set B) incorporated the same Xk 03–0517 platform but included an additional separating wagon positioned between the platform and the DH–350.11 rail vehicle (Fig. 2).

Fig. 1. Mobile measurement set in variant A

Fig. 2. Mobile measurement set, variant B

The measurement platform Xk 03–0517, with buffers, has an overall length of 12.240 m. It is constructed as a two-bogie vehicle, each bogie equipped with two axles and flanged wheels, and it operates without an independent propulsion system. The platform has a mass of 17,850 kg. The second element of the diagnostic set is the DH-350.11 hydraulic rail vehicle, measuring 12 m in length and equipped with a 350 kW drive engine, capable of reaching a maximum speed of 80 km/h.

In measurement set A, vibration signals were acquired using two 4504A triaxial accelerometers in combination with a 3050-A-060 B&K signal recording unit. Data were sampled at a frequency of 51.2 kHz. The accelerometers were mounted on the bearing housings (axle boxes) of the second wheel of the first bogie, on both the left and right sides of the rail platform (Fig. 1).

Measurements were collected along three orthogonal directions:

x-axis: aligned with the longitudinal direction of vehicle motion,

y-axis: transverse to the vehicle's motion in the horizontal plane,

z-axis: vertical to the track, perpendicular to both the wheelset axis and the railway line.

The signal recording cassette was installed on the measurement platform itself and remotely controlled via Wi-Fi using a mobile phone interface (Fig. 3a).

Measurement set B consisted of two single-axis transducers of type 4508 and a signal recording cassette of type 7533 B&K. The single-axis transducers were mounted under the upper shelf of the side part of the axle box on the second wheel of the first bogie (in the direction of travel of the railway platform) on both sides of the railway platform (Fig. 2). Vibration signals were recorded in the z direction - vertical to the movement of the rail vehicle, separately for the right and left wheels. The signal recording cassette was placed on the measurement platform and con- trolled from a computer via LAN (Fig. 3b).

Measurement set B comprised two 4508-type single-axis accelerometers coupled with a 7533 B&K signal recording unit. The accelerometers were installed beneath the upper shelf of the lateral section of the axle box on the second wheel of the first bogie, aligned with the direction of platform travel, and mounted symmetrically on both sides of the railway platform (Fig. 2).

Vibration signals were captured in the z-direction—perpendicular to the rail vehicle's motion—independently for the right and left wheels. The recording unit was positioned on the measurement platform and operated remotely via a computer connection through LAN (Fig. 3b)

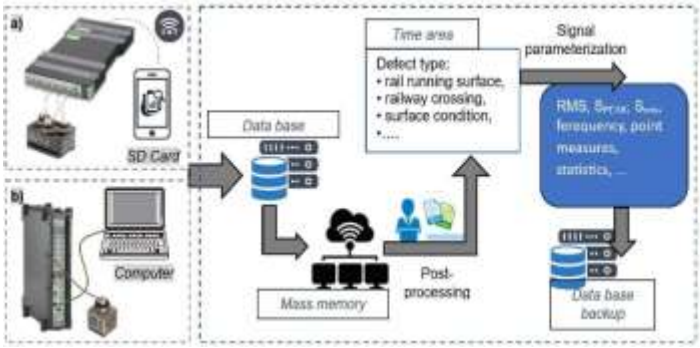

Fig. 3. Scheme of the architecture system for collecting and processing measurement data

In the subsequent stage, the pre-processed signals are **parameterized** separately for each vibration direction recorded from the two wheels of the vehicle. Signal parameterization, with respect to vibration directions, involves extracting characteristic features that are indicative of specific track surface conditions. In measurement variant (a), six vibration signals are available, enabling a broader spectrum of directional analyses compared to variant (b), which is limited to two signals. The results obtained from the parameterization process are then stored in a **backup database**, where they are systematically categorized into entities representing different defect types.

2. Data Processing Algorithms

This study examines three specific diagnostic cases: a) the identification of squat defects, b) the evaluation of railway crossing conditions in relation to the type of surface used, and c) the assessment of track surface conditions with consideration of fastening types and sleeper materials. The results of these analyses are presented in **Sections 4.1–4.3**. The corresponding data processing models are illustrated in **Figure 6**. For each case, a dedicated model was employed, enabling the determination of whether vibration signals can reliably support diagnostic identification.

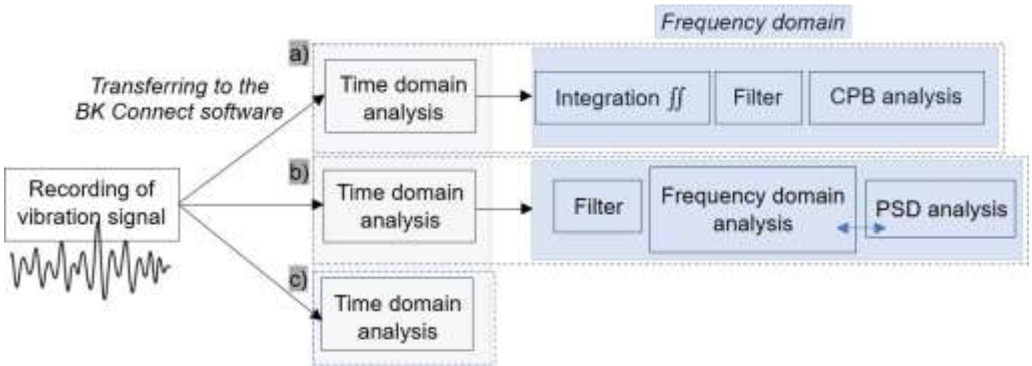

Fig. 4. Algorithm of data processing

In this study, the identification of rail surface defects (Fig. 5a) focused on detecting squat defect No. 227 from the official catalog of Polish Railway Lines. The recorded vibration signals were sampled at 51.2 kHz, ensuring sufficient resolution for subsequent spectral analysis. The operational frequency ranges of the 4504A vibration transducers were: x-axis: 1–11,000 Hz; y-axis: 1–9,000 Hz; z-axis: 1–18,000 Hz. Consequently, the Nyquist criterion was fulfilled for each axis,

Formally, the first and second derivatives of displacement x(t) with respect to time yield velocity (Eq. 1) and acceleration (Eq. 2), respectively:

$$v(t) = x'(t) \qquad (1)$$

$$a(t) = x''(t) \qquad (2)$$

where:

x(t) - displacement as a function of time,

v(t) - velocity as a function of time, the first derivative of displacement x(t) [m/s],

a(t) - acceleration as a function of time, the second derivative of displacement x(t) [m/s^2].

After performing a double integration of the vibration signal to obtain the corresponding vertical displacement, the next stage involved applying filtering techniques aimed at eliminating unwanted frequency components and suppressing noise. Since filtering operations are generally more effective in the frequency domain, the signals were transformed from the time domain to the frequency domain prior to processing.

This transformation was achieved using the Fast Fourier Transform (FFT), which converts a discrete time signal $x(n)$ into its frequency spectrum $X(k)$ according to the following expression:

$$X(k) = \sum_{n=0}^{N-1} x(n)e^{-j\frac{2\pi}{N}kn} \quad (3)$$

where:

X(k) - value of the Fast Fourier Transform at fre- quency k (k=0,1,…,N-1),

x(n) - sample of displacement signal in the time do- main,

N - number of samples of the vibration signal,

j - imaginary unit ($j^2 = -1$).

After transforming the vibration signals into the frequency domain, a dedicated filtering procedure was applied. To enhance the amplitude of the waveform and eliminate low-frequency noise, a high-pass Infinite Impulse Response (IIR) filter was implemented, providing an accuracy level of approximately 0.1 dB. The primary function of the high-pass filter was to suppress the DC component and mitigate low-frequency drift. However, this approach introduced a reduction in accuracy for frequencies below fs/3000f_s / 3000fs/3000. Considering a squat defect analysis, where low-frequency components (up to 100 Hz) are of diagnostic significance, this resulted in diminished accuracy within the 0–6.7 Hz range.

3. Analysis of Research Results

3.1. Application of Vibration Signal Analysis for the Identification of Squat Defects on the Running Surface – a Case Study

An example of the squat defect No. 227 is illustrated in Figure 6a. Squats typically appear on the running surface of the rail and are initially manifested through localized peeling and microcracking of the material, forming a characteristic semicircular “dimple.” The evolution of this defect is highly dependent on the specific operational and loading conditions of the railway line. As a point-type surface irregularity, the squat defect can significantly influence vehicle dynamics and safety. Its presence compromises the structural integrity of the track–vehicle interaction system, reduces overall operational reliability, and deteriorates ride comfort. In addition to squat defects, railway infrastructure is also affected by sectional surface anomalies such as wheel burns, which can extend over lengths of up to 1.5 meters

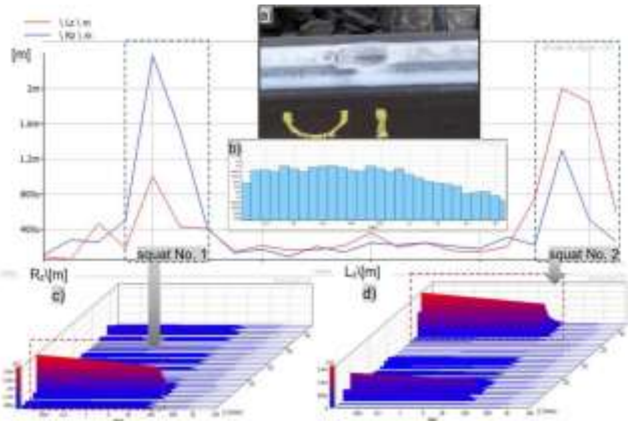

Fig. 5. Results of the analysis of the signal recorded at the squat defect: a – squat, b – CPB analysis, c,d - spectrum analysis for the vibration signal vertical direction for the right Rz and left Lz wheels

3.2. Evaluation of Railway Crossing Surface Conditions – Case Study

During the time-domain analysis of the vibration signal, an impulse-averaging method was employed, which enabled a precise examination of short-term variations occurring as the vehicle passed over a structural discontinuity, such as a crossing zone. The observed vibration acceleration amplitudes were notably higher for crossings with small-format slabs, reaching up to 40 m/s², while for crossings with CBP slabs, the amplitudes did not exceed 16 m/s²

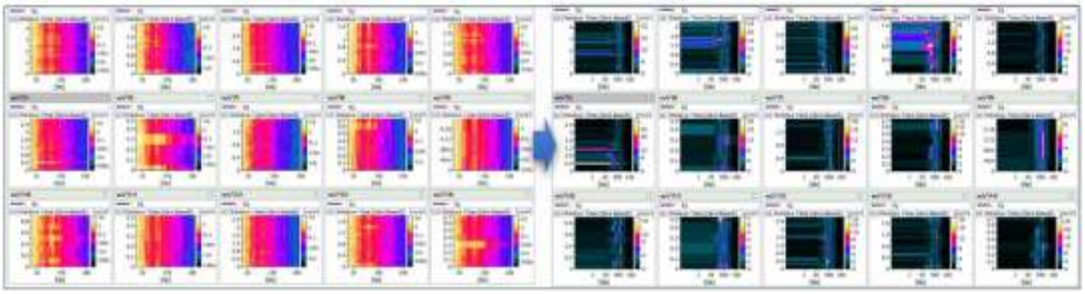

Fig. 6. Identification of the frequency trace resulting from the train's entry and exit from the railway crossing

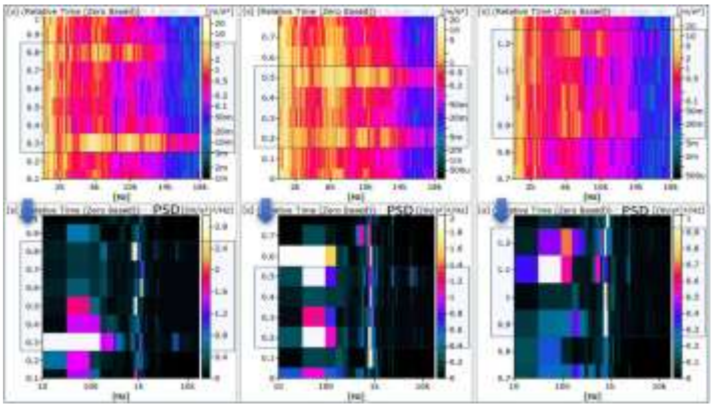

Fig. 7. Frequency spectrum and power spectral density for CBP slabs in the Lz vibration signal recording direction

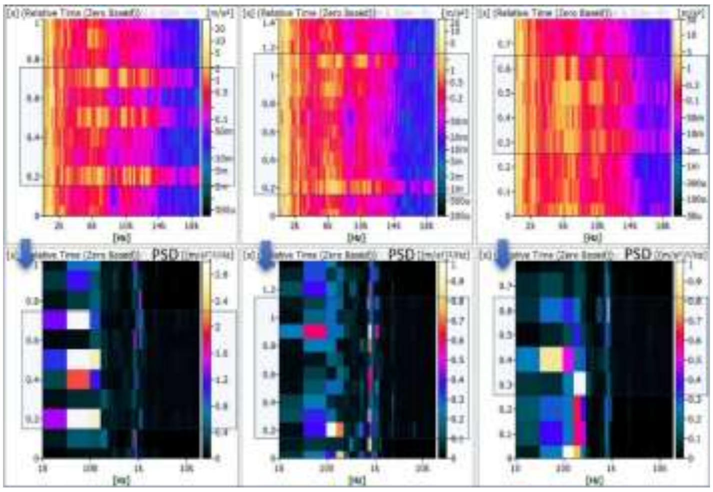

Fig. 8. Frequency spectrum and power spectral density for small sized slabs in the Lz vibration signal re- cording direction

Through the application of Power Spectral Density (PSD) analysis, it was possible to determine the distribution of signal energy in the frequency domain over the course of the vehicle's passage. The PSD results revealed that the regions corresponding to the entry and exit phases of the railway crossing exhibited the highest power levels throughout the entire observation window. The maximum spectral power was consistently observed around 200 Hz, regardless of the surface configuration. Moreover, elevated power levels were recorded within a narrow band near 800 Hz for crossings equipped with CBP slabs, and within the 700–900 Hz range for those utilizing small-sized slab elements. Further frequency-domain analysis demonstrated that the vibration spectra in both the vertical (z) and horizontal (y) directions featured distinctive amplitude characteristics. In the vertical direction, the dominant vibration acceleration amplitude reached approximately 10 m/s^2, while in the horizontal direction it averaged 2.5 m/s^2, both centered around 200 Hz. Additionally, secondary horizontal vibration components of roughly 1 m/s^2 were identified near 2000 Hz. A detailed examination of vibration signals recorded during crossings with small-sized slabs (within the track) and asphalt layers (on the outer sides) confirmed the presence of symmetrical amplitude peaks, similar to those identified for CBP slab crossings.

The spectral analysis (Figure 11b) focused on two representative cases of track surface transitions, analyzed exclusively along the vertical recording direction relative to the movement of the railway vehicle, and examined independently for the left (Lz) and right (Rz) wheel positions. Two sample signals—Signal 1 and Signal 2—were selected for comparative evaluation

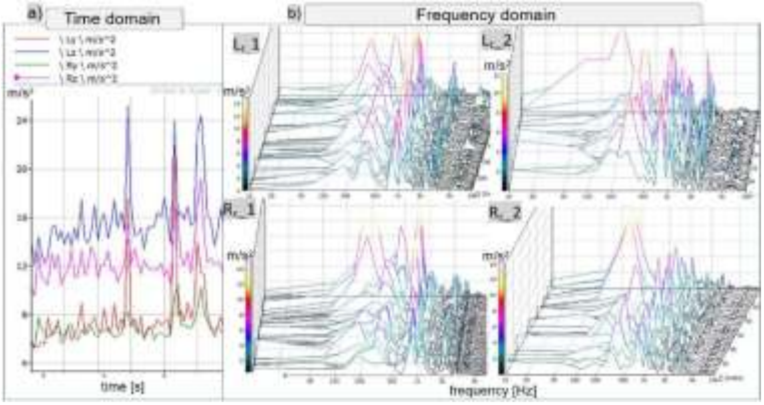

Fig. 9. Spectrum signal when changing the surface with wooden sleepers to concrete sleepers, where Lz_1 – vibration spectrum of signal No. 1 for the left wheel in the direction vertical to the vehicle movement; Lz_2 - vibration spectrum of signal No. 2 for the left wheel in the direction vertical to the vehicle movement; Rz_1 - vibration spectrum of signal No. 1 for the right wheel in the direction vertical to the vehicle movement; Rz_2 - vibration spectrum of signal No. 2 for the right wheel in the direction vertical to the vehicle movement

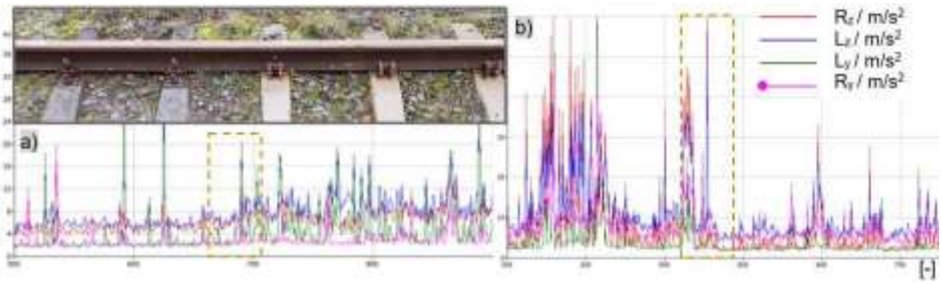

Fig. 10. Vibration signal when changing the type of fastening on concrete sleepers

Conclusion

The outcomes obtained in this study form a conceptual and methodological foundation for subsequent investigations across multiple domains of railway infrastructure diagnostics — including assessments of rail and level crossings and the continuous monitoring of track geometry and surface conditions. The application of vibration-based approaches to detect specific track irregularities has already been successfully demonstrated in onboard diagnostic systems, such as those employed in Japanese railway operations. The results of this research confirm the high diagnostic value of vibration signals, particularly when coupled with advanced post-processing methods aimed at the identification of localized surface and structural defects. A comprehensive synthesis of the conducted experiments indicates that each diagnostic scenario within railway systems requires customized analytical techniques and dedicated tools. For instance, in the evaluation of rolling surface defects such as squats, the most relevant diagnostic parameter involves tracking vertical displacement components of vibration signals within the low-frequency range up to approximately 200 Hz. Meanwhile, the examination of railway crossings relies on the analysis of power spectral density of vibrations measured both vertically and laterally relative to the vehicle's direction of travel, particularly in the 200–800 Hz range. In contrast, investigations concerning track surface transitions reveal the necessity of examining vibration signals within a broader spectral range, extending up to 15,000 Hz, to capture the full dynamic response of the rail structure.

References

1. Arcieri, G., Hoelzl, C., Schwery, O., Straub, D., Papakonstantinou, K. G., & Chatzi, E. (2024). POMDP inference and robust solution via deep reinforcement learning: An application to railway optimal maintenance. *Machine Learning*, 1-29. https://doi.org/10.1007/s10994-024-06559-2.
2. Arcieri, G., Rigoni, T., Hoelzl, C., Haener, D., Chatzi, E. (2024). Zurich, E. T. H., & SBB, S. F. R. Ground penetrating radar for moisture assessment in railway tracks: An experimental investigation. *Journal of Physics Conference Series.* https://doi.org/ 10.58286/29747.
3. Avci, O., Abdeljaber, O., Kiranyaz, S., Hussein, M., Gabbouj, M., & Inman, D. J. (2021). A review of vibration-based damage detection in civil structures: From traditional methods to Machine Learning and Deep Learning applications. *Mechanical systems and signal processing*, 147, 107077.

https://doi.org/10.1016/j.ymssp.2020.107077.

4. Barbosa, B., Serrador, A., & Casaleiro, J. (2023). Condition Monitoring Maintenance in Train Bogie: A Low-Cost Acceleration Sensor Proposal. *In 2023 International Conference on Control, Automation and Diagnosis (ICCAD)* (1-4). IEEE. https://doi.org/10.1109/ICCAD57653.2023.10152337.
5. Carnevale, M., La Paglia, I., & Pennacchi, P. (2021). An algorithm for precise localization of measurements in rolling stock-based diagnostic systems. *Proceedings of the Institution of Mechanical Engineers, Part F: Journal of Rail and Rapid Transit*, 235(7), 827-839. https://doi.org/10.1177/0954409720965798.
6. Chrzan, M. (2022). Effect of uniform time on the transmission of signals in rail open systems. *Archives of Transport*, 61(1), 39-49. https://doi.org/10.5604/01.3001.0015.8150.
7. Chudzikiewicz, A., & Kostrzewski, M. (2013). Analiza sygnałów wibroakustycznych w procesie monitorowania stanu zawieszenia pojazdów szynowych oraz toru. *Pojazdy Szynowe*, 1(2013), 10-17. https://doi.org/10.53502/RAIL-139165.
8. De Rosa, A., Alfi, S., & Bruni, S. (2019). Estimation of lateral and cross alignment in a railway track based on vehicle dynamics measurements. *Mechanical Systems and Signal Processing*, 116, 606-623. https://doi.org/10.1016/j.ymssp.2018.06.041.
9. Di Summa, M., Griseta, M. E., Mosca, N., Patruno, C., Nitti, M., Renò, V., & Stella, E. (2023). A review on deep learning techniques for railway infrastructure monitoring. *IEEE Access*. https://doi.org/10.1109/ACCESS.2023.3309814.
10. Faccini, L., Karaki, J., Di Gialleonardo, E., Somaschini, C., Bocciolone, M., & Collina, A. (2023). A methodology for continuous monitoring of rail corrugation on subway lines based on axlebox acceleration measurements. *Applied Sciences*, 13(6), 3773. https://doi.org/10.3390/app13063773.